Research Article | Vol. 29, No. 20 / 27 Sep 2021 / Optics Express 32682
Optics EXPRESS

Modal dynamics in multimode optical fibers: an attractor of high-order modes

WEITAO HE,[1] RUIHUAN WU,[1] WEIYI HONG,[1,2] AND AIPING LUO[1,3]

[1]Guangdong Provincial Key Laboratory of Nanophotonic Functional Materials and Devices, South China Normal University, Guangzhou 510631, China
[2]hongwy@m.scnu.edu.cn
[3]uoaiping@scnu.edu.cn

Abstract: Multimode fibers (MMFs) support abundant spatial modes and involve rich spatiotemporal dynamics, yielding many promising applications. Here, we investigate the influences of the number and initial energy of high-order modes (HOMs) on the energy flow from the intermediate modes (IMs) to the fundamental mode (FM) and HOMs. It is quite surprising that random distribution of high-order modes evolves to a stationary one, indicating the asymptotic behavior of orbits in the same attraction domain. By employing the Lyapunov exponent, we prove that the threshold of the HOMs-attractor is consistent with the transition point of the energy flow which indicates the HOMs-attracotr acts as a "valve" in the modal energy flow. Our results provide a new perspective to explore the nonlinear phenomena in MMFs, such as Kerr self-cleaning, and may pave the way to some potential applications, such as secure communications in MMFs.

1. Introduction

In recent years, multimode fibers (MMFs) are extensively investigated due to the great potential in spatial division multiplexing systems and multimode fiber lasers [1,2]. Meanwhile, MMFs offer larger mode areas, support more spatial modes, and provide a new degree of freedom to control the optical field [3]. MMFs involve complex spatiotemporal dynamics and intrinsic disorder, and they have been used to investigate a series of new nonlinear spatiotemporal dynamics phenomena, such as spatiotemporal mode-locking [4–7],multimode solitons [1,8,9], intermodal four-wave mixing [10–12], geometric parametric instability [13–17], spatiotemporal modulation instability [18], and Kerr beam self-cleaning [3,19–23]. These phenomena are of great interest not only from the point of view of basic science, but also in various practical applications [24].

As is known to all, optical field propagation in MMFs involves rich spatiotemporal dynamics and complex intermodal interactions [2,25,26]. More theoretical studies and ways are needed for a more profound understanding of complex spatiotemporal dynamic behaviors [25]. Control of physical phenomena in MMFs and their applications are in their infancy, opening opportunities to take advantage of complex nonlinear modal dynamics [27]. So far, although the physical mechanism of the Kerr beam self-cleaning phenomenon is an open problem, researchers have introduced concepts from different fields to provide a very constructive explanation: E. V. Podivilov et al. pointed out that Kerr beam self-cleaning is an analogue to wave condensation that is well known in hydrodynamic 2D turbulence [21,28], A. Picozzi proposed that condensation of light waves in MMFs is originates in the equilibrium Rayleigh-Jeans statistics of classical waves [29–31]. These research methods have offered some interesting ways and ideas for exploring the dynamic process in MMFs and opening up a new visual field.

The studies of E. V. Podivilov et al. showed that in the process of the mode energy transmission, the energy of the intermediate modes (IMs) flows into the fundamental mode (FM) and high-order modes (HOMs), which is analogous to the hydrodynamic 2D turbulence [21] and therefore contains rich physical phenomena. The HOMs with much lower energy compared to those of

#438798 https://doi.org/10.1364/OE.438798
Journal © 2021 Received 26 Jul 2021; revised 19 Sep 2021; accepted 19 Sep 2021; published 24 Sep 2021

Optics EXPRESS

FM and IMs act as the background noise but play an important role in the modal energy flow. In this letter, we systematically study the energy flow in the graded-index MMFs, and find that small modal number and tiny energy of the HOMs trigger the energy flow from the IMs to the FM and the HOMs. Quite surprisingly, the energy flow exhibits an attractor of the HOMs: random modal energy distribution of HOMs evolves to the stationary one, and such stationary distribution of the HOMs depends on the initial energy distribution of the FM and IMs. We further adopt the Lyapunov exponent to demonstrate the forming process of the HOMs-attractor, and find that initial energy proportion of HOMs determines the threshold of the HOMs-attractor. Interestingly, this threshold is consistent with the transition point of the energy outflow from the IMs, suggesting that the HOMs-attractor is a "valve" for the modal energy flow.

2. Numerical model

In MMFs, the description of pulse propagation often involves spatial and temporal dynamics at the same time. The modal decomposition translates to higher accuracy, and makes a clear interpretation of spatiotemporal dynamics in MMFs compared with the 3D nonlinear Schrödinger equation (NLSE) [30]. We numerically solve the generalized multimode nonlinear Schrödinger equation (MM-GNLSE) [2,32,33] to explore the process of modal dynamics in the following. The evolution of the electric field temporal envelope of the spatial mode p versus the propagation distance z can be written as:

$$\begin{aligned}
&\partial_z A_p(z,t) = \\
&i\delta\beta_0^{(p)} A_p - \delta\beta_1^{(p)}\partial_t A_P + \sum_{m=2}^{N_d} i^{m+1}\frac{\beta_m^{(p)}}{m!}\partial_t^m A_p + \\
&i\frac{n_2\omega_0}{c}(1+\frac{i}{\omega_0}\partial_t)\sum_{l,m,n}^{N}[(1-f_R)S^K_{plmn}A_l A_m A_n^* + \\
&f_R S^R_{plmn} A_l \int_{-\infty}^{t} d\tau h_R(\tau) A_m(z,t-\tau) A_n^*(z,t-\tau)],
\end{aligned} \tag{1}$$

where the first term, the second term and the third term on the right hand side indicate the propagation constant mismatch, the modal dispersion and the higher order dispersion effects, respectively. In the fourth term, n_2 represents the nonlinear refractive index, f_R shows the fractional contribution of the Raman effect ($f_R = 0.18$ in fused silica), h_R is the Raman response of the fiber medium, S^K_{plmn} and S^R_{plmn} are the modal overlap factors responsible for the Raman and Kerr effect severally [31].

3. Simulation and analysis

3.1. Modal energy flow

We launched Gaussian pulses with the duration of 50 fs, the wavelength of 1064 nm, and the initial total energy of 25 nJ into a 0.5-m-long graded-index MMF. The core radius of the fiber is 25 μm, the nonlinear index of refraction n_2 is $3.2\times10^{-20}m^2W^{-1}$ and the refractive index of the core is 1.4626, and the value of the refractive index difference is 0.013. In the dynamics of the modal energy flow, the energy of the IMs flows into the FM and the HOMs as shown in Fig. 1. In the following discussion, we regard the second to the fifth modes as the IMs and the next high-order modes as the HOMs. Firstly, we set the equal energy to the first five modes and the initial average energy ratio of E_{AEH}/E_{AEF} to 1/1000 (marked the E_{AEH} and E_{AEF} as the initial average energy of the HOMs and the initial average energy of the first five modes, respectively). Figure 1(a) shows the energy exchanges among the 30 spatial modes with the increase of propagation distance. These three-dimensional beam intensity models represent the

Optics EXPRESS

FM, IMs and HOMs at the input and output end of the fiber, respectively. In Fig. 1(b), the solid curves and dotted curves severally represent the energy flows where the HOM number is 25 and 0 in the initial field. Obviously, abundant energy flows from the IMs to the FM and HOMs when the HOMs are excited in the initial field. Figure 1(c) presents the relationship between the peak power and the rate of outflow of the IMs (the energy flowing out of the IMs divided by the initial energy of the IMs). The rate rises up and tends to saturate at the value of the input peak power is around 450 kW.

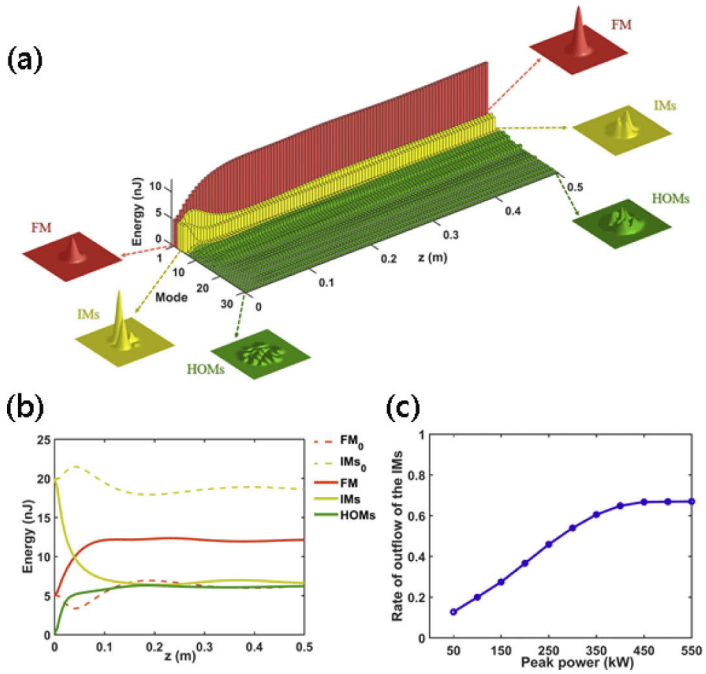

Fig. 1. (a) Evolutions of the fundamental mode (FM), intermediate modes (IMs) and higher-order modes (HOMs) upon the propagation distance z. Illustrations represent the beam intensity patterns at the input and output end of the fiber, respectively. (b) Energy flows of the FM, IMs and HOMs where z is 0.5 m. Dotted curves indicate the case that there is no HOMs in the initial field. (c) The rate of outflow of the IMs at the output end of the fiber versus the peak power. The input peak power is 500 kW for (a) and (b).

Since the noise background formed by the HOMs leads to the energy flow from IMs to the FM and the HOMs, the modal number and the energy proportion of the HOMs would naturally influence this process. We show in Fig. 2(a) the difference between the output and input energies for both FM and HOMs as functions of the HOM number. The average of them implies the total energy flow from the IMs. It is interesting that very small number of HOMs significantly triggers the energy flow, and the energy flow from the IMs saturates immediately as the HOMs number increases. The energy which flows to the HOMs exhibits a slow decrease after its sharp increase. The insets (i) and (ii) representing the spot of the total output field depict the beam cleaning improved by the HOMs. We keep the HOM number of 30 which is within the saturation region as shown in Fig. 2(a), and investigate the influence of the initial energy of the HOMs on the energy flow. Figure 2(b) shows that extremely weak noise background of the HOMs is enough to trigger the energy flow. As the initial energy of the HOMs increases, the energy flow from the IMs keeps unchangeable and significantly declines when initial energy proportion of the HOMs reaches a certain value of $E_{AEH}/E_{AEF} = 1/50$. It is worth mentioning that the energy flow to the

Optics EXPRESS

HOMs experiences a rise and reach its maximum also at $E_{AEH}/E_{AEF} = 1/50$. We will see below that it is the transformation point of the HOMs. The insets (i) and (ii) also imply that weaker energy of the HOMs facilitates the beam cleaning.

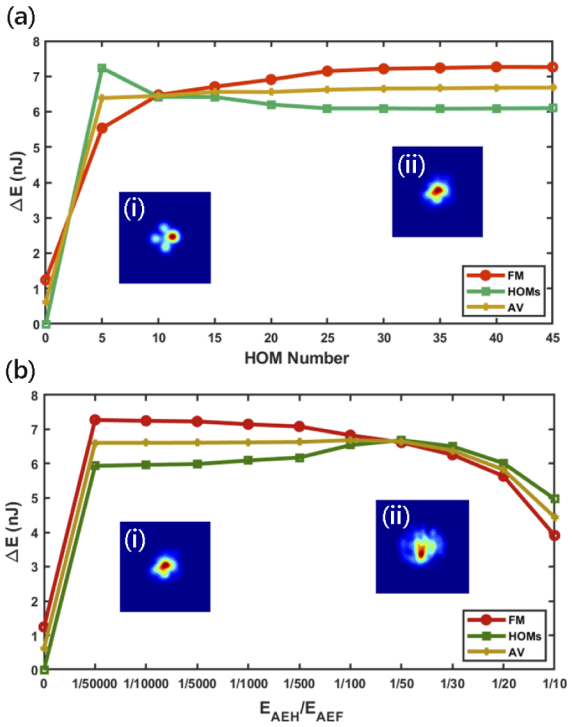

Fig. 2. (a) Energy difference between the output and input energies versus the HOM number (the ratio of the E_{AEH} to the E_{AEF} is 1/1000). Inset: (i) and (ii) correspond to the output beam profiles where the HOM number is 0 and 45, respectively. (b) Energy difference between the output and input energies for the varying ratios of the E_{AEH} to the E_{AEF} (the HOM number is set to 30). Inset: (i) and (ii) correspond to the output beam profiles where the ratio are severally 1/50,000 and 1/10. AV is the average value of the energy variations of the FM and HOMs. In order to keep the peak power (500 kW) and the initial energy of the first five modes unchanged, we increased the total input energy and pulse width appropriately.

3.2. HOMs-attractor

Previous studies for the modal energy flow always focused on the energy flow to the FM, i.e., the beam cleaning, due to the its applications of bright FM beam generation. Quite different from the previous studies, we focus on the evolution of the energy distribution of the HOMs in the modal energy flow, and find a very surprising phenomenon: *the dynamics of the HOMs exhibit an attractor*. Figure 3(a) illustrates that two *random* initial energy distributions of the HOMs (respectively marked as Input 1 and Input 2) evolve to the same distribution after the propagation of the 0.5-m long fiber. In this simulation, the energies of the FM and IMs (the lowest five modes) are assumed to be the same value of 5 nJ and the energy proportion of the HOMs is set to $E_{AEH}/E_{AEF} = 1/50000$. To avoid coincidence, we have examined this process by multiply randomizing the distribution of HOMs. In other words, random distribution of the HOMs will evolve to a stationary one. Note that the initial energies of the FM and IMs and initial average energy of the HOMs are fixed in the simulation, therefore we could reasonably conjecture the existence of an attractor of HOMs in the phase space constructed by the modal energies. We

Optics EXPRESS

further perform the simulation with the same parameters as those in Fig. 3(a) but for different energy distribution of the lowest five modes. As expected, random distribution of the HOMs in Fig. 3(b) evolves to the attractor different from that in Fig. 3(a). Therefore, it can be concluded that such attractor of HOMs depends on the initial energy distribution of the FM and IMs, and also the total energy proportion of the HOMs.

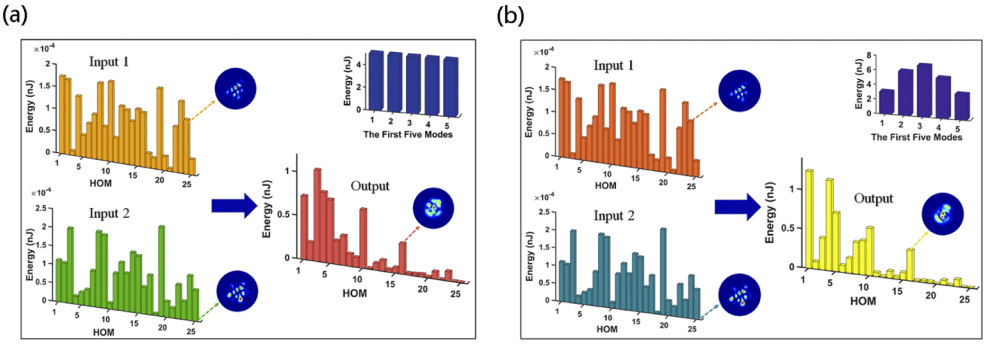

Fig. 3. The numerical evolution results of the 25 HOMs with different initial energy distributions of the first five modes (the input peak power is also 500 kW). (a) Input 1 and input 2 represent two different random initial energy distributions of the HOMs. The outputs of input 1 and input 2 are the same and the three beam profiles in this figure correspond to the input 1, input 2 and output, respectively. (b) Same conditions as (a) except for the initial energy distribution of the first five modes (0.12, 0.24, 0.28, 0.22, 0.14).

Based on the above numerical results for the evolution of the HOMs which evolve the behavior of the attractors, we would like to further schematically demonstrate the concept of such attractor in the phase space constructed by the mode energies. The attractor is regarded as the asymptotic behavior of orbits, which originates from the topological properties of differential equations [34]. Figure 4(a) depicts the orbits for two attractors in the phase space $\Omega[E_1, E_2, E_3, E_4, E_5, E_{AEH}]$. $S_1(E^1_{1-5}, E^1_{AEH})$ and $S_2(E^2_{1-5}, E^2_{AEH})$ are two different states in Ω. They evolve along their own

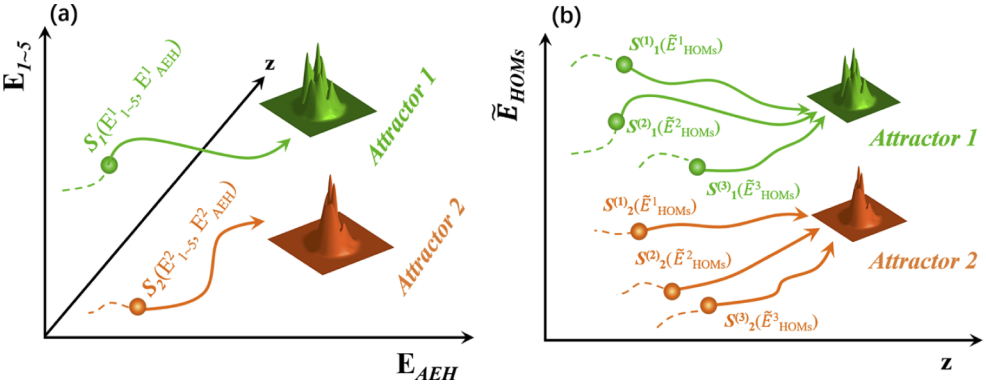

Fig. 4. Schematic diagram of the attractors of HOMs. (a) A six-dimensional phase space consisting of the energies of the first five modes (E_1, E_2, E_3, E_4, E_5) and the HOMs (E_{AEH}). Two different states (S_1 and S_2) respectively evolve along their own orbits towards corresponding attractors which are determined by the initial energy distributions of the first five modes. (b) Three different sub-states ($S_1^{(1)}$, $S_1^{(2)}$, $S_1^{(3)}$) which have the same the initial energy distributions of the first five modes evolve towards the same attractor (Attractor 1) and the orther three evolve towards another attractor (Attractor 2).

Optics EXPRESS

inherent orbits (marked by the arrows) and tend asymptotically to the corresponding attractors. Although these two states in the actual light propagation in the fiber may be the initial conditions, they could be the intermediate states in the orbits, rather than being regarded as the beginning of the orbits. It should be mentioned that any state in Ω can only evolve along an exclusive orbit to its corresponding attractor, and any two orbits never intersect in Ω.

It could be vivid to see the behavior of the attractor in sub-space $l[\widetilde{E}_{HOMs}]$ constructed by the modal energies of HOMs ($\widetilde{E}_{HOMs}$ represents the series of the energies of HOMs normalized by E_{AEH}), which is shown in Fig. 4(b). In l, three different sub-states $S_1^{(1)}(\widetilde{E}_{HOMs}^1)$, $S_1^{(2)}(\widetilde{E}_{HOMs}^2)$ and $S_1^{(3)}(\widetilde{E}_{HOMs}^3)$, which are all belong to the state S_1 in Ω since their initial energies of the first five modes and the intial average energy of the HOMs are the same, will evolve asymptotically along their own sub-orbits to the same state (marked as Attractor1). And the same goes for another three sub-states $S_2^{(1)}(\widetilde{E}_{HOMs}^1)$, $S_2^{(2)}(\widetilde{E}_{HOMs}^2)$ and $S_2^{(3)}(\widetilde{E}_{HOMs}^3)$.

4. Results and discussion

Lyapunov exponent [35–37] would be helpful to deeply investigate the behavior of attractor demonstrated above, which can be expressed as follows:

$$\lambda_{LE} = \lim_{L\to\infty} \frac{1}{L} \ln \frac{\left\| S_{z=L}^{(2)} - S_{z=L}^{(1)} \right\|_2}{\left\| S_{z=0}^{(2)} - S_{z=0}^{(1)} \right\|_2}, \tag{2}$$

where $S^{(1)}$ and $S^{(2)}$ are two sub-states in l, and are both belong to the state S in Ω, and L is the propagation distance of the fiber. $\| * \|_2$ denotes the 2-norm in l. When λ_{LE}<0, the system exhibits a behavior of attractor, otherwise the system is chaotic. Although L should tend to infinite in the definition of λ_{LE}, it can be sufficiently long where the energy flow tend to be saturated in the practical simulations. We assume the parameters for the state S as Fig. 3(a) and calculate the spectrum of its Lyapunov exponent $\lambda_{LE}(d)$ with $d = \|S^{(2)} - S^{(1)}\|_2$ the 2-norm, i.e., the distance of two initial sub-states. As shown in Fig. 5(a), λ_{LE} is always near −5.85 with a slight rise as d_0 (initial distance of two adjacent sub-orbits) increases from 0.01 to 0.1.

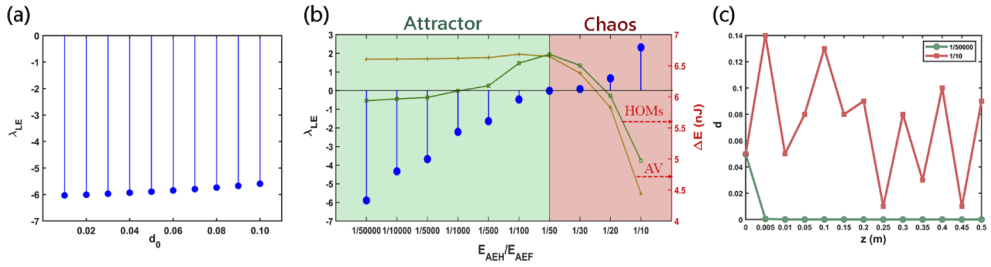

Fig. 5. (a) Correlation between the Lyapunov exponent and the different initial distance of two orbits. (b) The Lyapunov exponent and the energies difference of the HOMs and AV (same as Fig. 2(b)) for the varying ratios of the E_{AEH} to the E_{AEF}). This area is divided to the Attractor and Chaos based on the positive and negative values of the Lyapunov exponent. (c) The normalized distance d of the two orbits upon the propagation distance z for the attractor (1/50000) and chaos (1/10). The peak input power is maintained at 500 kW.

In Fig. 5(b), we further shift the state S along the axis E_{AEH} in the space of Ω shown in Fig. 4(a), and find that λ_{LE} tends to zero and subsequently becomes positive as the increases of E_{AEH}. The diminishing of $|\lambda_{LE}|$ for the attractor means that the system need longer propagation distance to converge to the attractor. The result also shows that the system exist a transformation point of the

Optics EXPRESS

attractor near $E_{AEH}/E_{AEF} = 1/50$. The spatial beam self-cleaning in MMFs originates from a universal unstable attractor, and once the critical state of the attractor is reached, the initial field will self-organizes into a stable state [18,26]. When the initial energy of the HOMs is very low, it can be regarded as a perturbation of the total initial field. Therefore, as the total initial field self-organizes into a stable state, the HOMs with random initial energy distribution will reach the same stable state. In other words, the orbits in the same attraction domain evolve into the same attractor. Conversely, when the initial energy of the HOMs is high, the field will evolve into a chaotic state due to the large disturbance. We also plot the energy flow from the IMs, and find that it keeps unchangeable within region where the attractor, and declines from the transformation point of the attractor, which implies that the HOMs-attractor is a "valve" for the energy flow from the IMs. The findings of the HOMs-attractors also lead to a deeper understanding of the generation for the Kerr self-cleaning in MMFs: the threshold is not only related to the input peak power, but also to the initial energy distribution of these modes. Based on our numerical results, we can conclude that the behavior of HOMs-attractor is general in common graded-index MMFs, rather than a multimode fiber with fixed parameters. We further calculate the evolution of the distance of two sub-states in the regions of attractor and chaos, respectively. As expected, the distance for the case of attractor reduces rapidly to zero as shown in Fig. 5(c), implying the fast merging of two adjacent sub-orbits, while that for the case of chaos fluctuates during propagation, implying the unpredictable behavior of the sub-orbits.

5. Conclusion

In conclusion, we systematically investigate the mode dynamics in the graded-index MMFs, and focus on the energy flow from IMs to FM and HOMs. It is found that small mode number and tiny energy proportion of HOMs significantly trigger the energy flow, and the mode number exhibits seldom influence on the energy flow when it is higher than 30. It is found a surprising phenomenon that the evolution of the HOMs exists the behavior of attractor when the energy proportion of the HOMs is under a certain value: random distribution of the HOMs evolves to a stationary one, and the attractor depends on the initial distributions of the FM and the IMs. Our results show that the HOMs-attractor acts as a "valve" in the modal energy flow, which may provide a new perspective to explore the nonlinear phenomena in MMFs, such as Kerr self-cleaning (which is thought useful for making high quality multimode fiber lasers). At present, mode recognition in multimode fibers can be experimentally realized using the so-call STRIPED FISH [38,39]. This pulse measurement technique will provide a helpful way for further experiment studies about the modal energy flow in MMFs. We further adopt Lyapunov exponent to quantitatively discuss the behavior of the attractor of HOMs. Base on such consistent one-to-one match between the input of FM and IMs and the output of the attractor of HOMs, this phenomenon might be applied on the area of secure communications.

Funding. Natural Science Foundation of Guangdong Province (2019A1515011172); National Natural Science Foundation of China (11874019, 61875058, 92050101).

Disclosures. The authors declare no conflicts of interest.

Data availability. No data were generated or analyzed in the presented research.

References

1. L. G. Wright, W. H. Renninger, D. N. Christodoulides, and F. W. Wise, "Spatiotemporal Dynamics of Multimode Optical Solitons," Opt. Express. **23**, 3492 (2015).
2. P. Horak and F. Poletti, "Multimode Nonlinear Fibre Optics: Theory and Applications," Recent Prog. Opt. Fiber Res. **1**, 3–24 (2012).
3. Z. Liu, L. G. Wright, D. N. Christodoulides, and F. W. Wise, "Kerr Self-Cleaning of Femtosecond-Pulsed Beams in Graded-Index Multimode Fiber," Opt. Lett. **41**, 3675 (2016).
4. H. Qin, X. Xiao, P. Wang, and C. Yang, "Observation of Soliton Molecules in a Spatiotemporal Mode-Locked Multimode Fiber Laser," Opt. Lett. **43**, 1982 (2018).

Optics EXPRESS

5. Y. Ding, X. Xiao, P. Wang, and C. Yang, "Multiple-Soliton in Spatiotemporal Mode-Locked Multimode Fiber Lasers," Opt. Express **27**, 11435 (2019).
6. L. G. Wright, P. Sidorenko, H. Pourbeyram, Z. M. Ziegler, A. Isichenko, B. A. Malomed, C. R. Menyuk, D. N. Christodoulides, and F. W. Wise, "Mechanisms of Spatiotemporal Mode-Locking," Nat. Phys. **16**, 565 (2020).
7. Y. Ding, X. Xiao, K. Liu, S. Fan, X. Zhang, and C. Yang, "Spatiotemporal Mode-Locking in Lasers with Large Modal Dispersion," Phys. Rev. Lett. **126**, 093901 (2021).
8. W. H. Renninger and F. W. Wise, "Optical Solitons in Graded-Index Multimode Fibres," Nat Commun **4**, 1719 (2013).
9. L. RishØj, B. Tai, P. Kristensen, and S. Ramachandran, "Soliton self-mode conversion: revisiting Raman scattering of ultrashort pulses," Optica **6**, 304 (2019).
10. E. Nazemosadat, H. Pourbeyram, and A. Mafi, "Phase Matching for Spontaneous Frequency Conversion via Four-Wave Mixing in Graded-Index Multimode Optical Fibers," J. Opt. Soc. Am. B **33**, 144 (2016).
11. R. Dupiol, A. Bendahmane, K. Krupa, A. Tonello, M. Fabert, B. Kibler, T. Sylvestre, A. Barthelemy, V. Couderc, S. Wabnitz, and G. Millot, "Far-Detuned Cascaded Intermodal Four-Wave Mixing in a Multimode Fiber," Opt. Lett. **42**, 1293 (2017).
12. A. Bendahmane, K. Krupa, A. Tonello, D. Modotto, T. Sylvestre, V. Couderc, S. Wabnitz, and G. Millot, "Seeded Intermodal Four-Wave Mixing in a Highly Multimode Fiber," J. Opt. Soc. Am. B **35**, 295 (2018).
13. K. Krupa, A. Tonello, A. Barthelemy, V. Couderc, B. M. Shalaby, A. Bendahmane, G. Millot, and S. Wabnitz, "Observation of Geometric Parametric Instability Induced by the Periodic Spatial Self-Imaging of Multimode Waves," Phys. Rev. Lett. **116**, 183901 (2016).
14. C. Mas Arabí, A. Kudlinski, A. Mussot, and M. Conforti, "Geometric Parametric Instability in Periodically Modulated Graded-Index Multimode Fibers," Phys. Rev. A **97**, 023803 (2018).
15. H. E. Lopez-Aviles, F. O. Wu, Z. Sanjabi Eznaveh, M. A. Eftekhar, F. Wise, R. Amezcua Correa, and D. N. Christodoulides, "A Systematic Analysis of Parametric Instabilities in Nonlinear Parabolic Multimode Fibers," APL Photonics **4**, 022803 (2019).
16. M. Conforti, C. Mas Arabi, A. Mussot, and A. Kudlinski, "Fast and Accurate Modeling of Nonlinear Pulse Propagation in Graded-Index Multimode Fibers," Opt. Lett. **42**, 4004 (2017).
17. W. H. E. J. Dai, Q. M. A. A. Luo, and W. Hong, "Modal perspective on geometric parametric instability sidebands in graded-index multimode fibers," Opt. Express **29**, 11353 (2021).
18. L. G. Wright, Z. Liu, D. A. Nolan, M.-J. Li, D. N. Christodoulides, and F. W. Wise, "Self-organized instability in graded-index multimode fibres," Nat. Photonics **10**, 771 (2016).
19. K. Krupa, A. Tonello, B. M. Shalaby, M. Fabert, A. Barthélémy, G. Millot, S. Wabnitz, and V. Couderc, "Spatial Beam Self-Cleaning in Multimode Fibres," Nat. Photonics **11**, 237 (2017).
20. O. S. Sidelnikov, E. V. Podivilov, M. P. Fedoruk, and S. Wabnitz, "Random Mode Coupling Assists Kerr Beam Self-Cleaning in a Graded-Index Multimode Optical Fiber," Opt. Fiber Technol. **53**, 101994 (2019).
21. E. V. Podivilov, D. S. Kharenko, V. A. Gonta, K. Krupa, O. S. Sidelnikov, S. Turitsyn, M. P. Fedoruk, S. A. Babin, and S. Wabnitz, "Hydrodynamic 2D Turbulence and Spatial Beam Condensation in Multimode Optical Fibers," Phys. Rev. Lett. **122**, 103902 (2019).
22. E. Deliancourt, M. Fabert, A. Tonello, K. Krupa, A. Desfarges-Berthelemot, V. Kermene, G. Millot, A. Barthélémy, S. Wabnitz, and V. Couderc, "Kerr Beam Self-Cleaning on the LP 11 Mode in Graded-Index Multimode Fibers," OSA Continuum **2**, 1089 (2019).
23. J. Lægsgaard, "Spatial Beam Cleanup by Pure Kerr Processes in Multimode Fibers," Opt. Lett. **43**, 2700 (2018).
24. S. K. Dacha and T. E. Murphy, "Spatiotemporal characterization of nonlinear intermodal interference between selectively excited modes of a few-mode fiber," Optica **7**, 1796 (2020).
25. P. Mondal, V. Mishra, and S. K. Varshney, "Nonlinear interactions in multimode optical fibers," Opt. Fiber Technol. **54**, 102041 (2020).
26. K. Krupa, A. Tonello, A. Barthélémy, T. Mansuryan, V. Couderc, G. Millot, P. Grelu, D. Modotto, S. A. Babin, and S. Wabnitz, "Multimode nonlinear fiber optics, a spatiotemporal avenue," APL Photonics **4**, 110901 (2019).
27. O. Tzang, A. M. Caravaca-Aguirre, K. Wagner, and R. Piestun, "Adaptive wavefront shaping for controlling nonlinear multimode interactions in optical fibres," Nat. Photonics **12**, 368 (2018).
28. F. O. Wu, A. U. Hassan, and D. N. Christodoulides, "Thermodynamic theory of highly multimoded nonlinear optical systems," Nat. Photonics **13**, 776 (2019).
29. A. Fusaro, J. Garnier, K. Krupa, G. Millot, and A. Picozzi, "Dramatic Acceleration of Wave Condensation Mediated by Disorder in Multimode Fibers," Phys. Rev. Lett. **122**, 123902 (2019).
30. K. Baudin, A. Fusaro, K. Krupa, J. Garnier, S. Rica, G. Millot, and A. Picozzi, "Classical Rayleigh-Jeans Condensation of Light Waves: Observation and Thermodynamic Characterization," Phys. Rev. Lett. **125**, 244101 (2020).
31. K. Baudin, A. Fusaro, J. Garnier, N. Berti, K. Krupa, I. Carusotto, S. Rica, G. Millot, and A. Picozzi, "Energy and wave-action flows underlying Rayleigh-Jeans thermalization of optical waves propagating in a multimode fiber," EPL **134**, 14001 (2021).
32. L. G. Wright, Z. M. Ziegler, P. M. Lushnikov, Z. Zhu, M. A. Eftekhar, D. N. Christodoulides, and F. W. Wise, "Multimode Nonlinear Fiber Optics: Massively Parallel Numerical Solver, Tutorial and Outlook," IEEE J. Sel. Top. Quantum Electron. **24**, 1 (2018).

Optics EXPRESS

33. F. Poletti and P. Horak, "Description of ultrashort pulse propagation in multimode optical fibers," J. Opt. Soc. Am. B **25**, 1645 (2008).
34. J. Milnor, "On the Concept of Attractor," Commun. Math. Phys. **99**, 177-195 (1985).
35. M. Bračič and A. Stefanovska, "Nonlinear Dynamics of the Blood Flow Studied by Lyapunov Exponents," Bull. Math. Biol. **60**, 417 (1998).
36. L. Arnold and V. Wihstutz, pp.1–26 in *Lyapunov Exponents. Proceedings. Bremen 1984*, L. Arnold and V. Wihstutz (eds.), Lecture Notes in Mathematics 1186, Springer, Berlin 1986
37. L. Barreira, Lyapunov exponents (Switzerland:Springer, 2017).
38. Gabolde Pablo and Trebino Rick, "Single-shot measurement of the full spatiotemporal field of ultrashort pulses with multispectral digital holography," Opt. Express **14**, 11460 (2006).
39. ZHU Ping, JAFARI Rana, JONES Travis, and TREBINO Rick, "Complete measurement of spatiotemporally complex multi-spatial-mode ultrashort pulses from multimode optical fibers using delayscanned wavelength-multiplexed holography," Opt. Express **25**, 24015 (2017).